JJMIE

Volume 11 Number 3, September. 2017
ISSN 1995-6665
Pages 147 -154

Jordan Journal of Mechanical and Industrial Engineering

Reduced Filtered Dynamic Model for Joint Friction Estimation of Walking Bipeds

Iyad Hashlamon * a, Kemalettin Erbatur b

[a] *Palestine Polytechnic University, Hebron, Palestine*
[b] *Faculty of Engineering and Natural Sciences, Sabanci University, Tuzla, Istanbul, Turkey*

Received 27 Jan, 2017 *Accepted April 5,2017*

Abstract

The present paper presents a novel method for estimating the joint friction of walking bipeds. It combines a measurement-based method with an adaptive model-based method to estimate the joint friction. The former is used when the feet is in contact, while the latter is used when the leg is swinging. The measurements are the feet forces and the readings of an inertial measure unit located at the biped body. The measurement-based method utilizes these measurements into a reduced filtered dynamic model of the biped to obtain an online estimated filtered version of the joint friction. Once the foot swings, a friction model is adopted to represent the joint friction behavior. The model parameters are adaptively identified using the online estimated filtered friction whenever the foot is in contact. The results are validated using full-dynamics of 12-DOF biped model and show a dramatic tracking of the estimated friction to the true one.

Keywords: *Humanoid robot, joint friction, CoM states, biped model.*

1. Introduction

The interest in the humanoid adaptive, efficient, and robust motion control is dramatically increased [1-7, 8]. However, the biped structure makes its dynamics highly nonlinear and hard to be stabilized. Another difficulty rises from the robot mechanical structure which makes the control challenge harder. Robots contain transmissions or drive mechanisms to transfer the power from the actuator to the robot link through the joint [9]. Therefore, friction is observed at the joints. Friction has a considerable effect on the robot behavior. It may deteriorate the robot walking performance. Typical consequences of joint friction are steady state errors, limit cycles and poor dynamic response [10, 11]. Therefore, joint friction compensation attracted the researchers' attention and interest [12, 13].

1.1. Related Work

Friction model-based method is intensively used for friction compensation. The friction behavior is represented using a mathematical model [14-17] and the model parameters are identified using offline identification methods [18-21]. However, the friction is environment and load dependant phenomenon [12, 22]. Therefore, adaptive identification methods were developed to identify the friction model parameters [23-27]. However, the friction is a complex phenomenon and representing it using a mathematical model is a challenge.

Friction modeling challenge was a strong motivation for the researchers to look for model-free methods. The friction is considered a disturbance along with external disturbances, system model uncertainty and so on. Then, a disturbance observer [28, 29] is used to reduce the effect of this disturbance [30-33]. Other studies used friction approximators based on soft computing techniques, such as Neural Networks (NN) and Fuzzy systems [24, 34-44]. However, approximation errors exist [45]. Model-free and measurement base method is reported too. Here the difficulty of friction modeling is avoided by mounting extra torque/force sensors on the robot. In [46, 47], the manipulator link torque is measured using a torque sensor and used in the feedback of the control loop. However, the sensors should be added in the design process. For fixed base robots, the base is equipped by a force/toque sensor to form the Base Sensor Control (BSC) method [22]. The sensor readings are mapped to the manipulator’s link to calculate the link torque which is used in the feedback torque control loop. However, the humanoid robot is mobile and not fixed in the ground.

1.2. Problem Importance and Definition

Joint friction is the major disturbance of the actuator and transmission unit at the joint. As a demonstration of joint friction effect for legged robots, refer to the video of some experiments conducted in the control system laboratory in Toyota technological institute [48].

Beyond the aforementioned consequences of joint friction, the compensation of joint friction is crucial for

* Corresponding author e-mail: iyad@ppu.edu.

some control techniques and locomotion in legged robots. In the absence of joint torque sensors, the joint torque is estimated using the transpose of the Jacobian for each leg. However, the accuracy of this method is not sufficient when joint friction is observed and not compensated [49, 50, 51].

To this end, joint friction for legged robots is either neglected [52-55], regarded as a disturbance and tried to be eliminated by a disturbance observer [30], or estimated using a friction model with offline identified parameters [56, 57]. Here, if the model parameters are known or identified with very small uncertainty then model-based method of joint friction estimation has better precision compensation [58]. On the other hand, high accuracy requires adaptive parameter tuning and, hence, information about the friction is required. The measurement-based method avoids friction modeling and approximation problems. However, it requires joint torque sensors. Furthermore, it is inapplicable directly to bipedal applications because, while walking, the biped switches its legs from the Double Support phase (DS) to the Single Support phase (SS), and so forth. Other challenges rise from the structure of the bipeds; its model includes the hard to measure body position and its derivatives in addition to the joint angles and their derivatives.

Therefore, a method is required to estimate the joint friction for walking biped. This method would have the advantages of the measurement-based and the adaptive model-based methods. It must be able to overcome the unmeasured variables limitations.

1.3. Proposed Method

The present paper proposes a new method for biped joint friction estimation. It combines the measurement-based method with the adaptive model-based method.

Measurement-based method is a method that works only when the foot is in contact with the ground and employs the biped model without friction models to estimate the joint friction. To accomplish this estimation, the joints angular accelerations, which are not measured directly, are required. The robot body (called base later on) velocity and orientation are estimated as in [59-61]. The explicit calculation of the joint angular accelerations is avoided by adopting the filtered dynamics model method [62]. Here, the biped model is reduced then filtered using a stable first order low pass filter to form the reduced filtered dynamical model of the biped. Then, the measured Ground Reaction Forces (GRF), the readings of Inertial Measurement Unit (IMU), and the estimated base velocity are utilized in the obtained reduced filtered dynamical model to estimate a filtered version of the joint friction online. However, when the GRF are no longer available (the foot is not in contact with the ground), the former estimation method is inapplicable. Therefore, a friction model is adopted to overcome this problem. The friction model is used only when the foot is not in contact with the ground and its parameters are adaptively identified whenever the foot is in contact with the ground.

The rest of the paper is organized as follows: Section **Error! Reference source not found.** describes the biped model. Friction estimation is derived in section **Error! Reference source not found.**Section **Error! Reference source not found.** presents the results. The paper conclusion is in Section (5).

2. Biped Model

For a biped with N number of joints, the robot model is:

$$\begin{pmatrix} H_{11} & H_{12} & H_{13} & H_{14} \\ H_{21} & H_{22} & H_{23} & H_{24} \\ H_{31} & H_{32} & H_{33} & 0 \\ H_{41} & H_{42} & 0 & H_{44} \end{pmatrix} \begin{pmatrix} \dot{\mathbf{v}}_b \\ \dot{\boldsymbol{\omega}}_b \\ \ddot{\boldsymbol{\theta}}_{\mathbf{L}} \\ \ddot{\boldsymbol{\theta}}_{\mathbf{R}} \end{pmatrix} + \begin{pmatrix} \mathbf{b_1} \\ \mathbf{b_2} \\ \mathbf{b_L} \\ \mathbf{b_R} \end{pmatrix} + \begin{pmatrix} \mathbf{u}_{\mathbf{F}_1} \\ \mathbf{u}_{\mathbf{F}_2} \\ \mathbf{u}_{\mathbf{F_L}} \\ \mathbf{u}_{\mathbf{F_R}} \end{pmatrix} = \begin{pmatrix} \mathbf{f}_b \\ \mathbf{n}_b \\ \boldsymbol{\tau}_{\mathbf{L}} \\ \boldsymbol{\tau}_{\mathbf{R}} \end{pmatrix} + \begin{pmatrix} \mathbf{u}_{\mathbf{E}_1} \\ \mathbf{u}_{\mathbf{E}_2} \\ \mathbf{u}_{\mathbf{E_L}} \\ \mathbf{u}_{\mathbf{E_R}} \end{pmatrix} \quad (1)$$

where $\boldsymbol{\theta} \in R^N$ and $\dot{\boldsymbol{\theta}} = \boldsymbol{\omega} \in R^N$ are the joint displacements and angular velocity vectors, respectively, $\boldsymbol{\theta}$ is measured using joint encoders attached to the joint actuators . $\mathbf{p}_b$ and $\dot{\mathbf{p}}_b = \mathbf{v}_b$ are the position and linear velocity of the robot base-link. $\dot{\mathbf{v}}_b$ and $\boldsymbol{\omega}_b$ are the acceleration and angular velocity of the robot body, respectively, they are measured using an IMU. $\mathbf{f}_b$ and $\mathbf{n}_b$ are the force and torque vectors at the base-link, and $\boldsymbol{\tau}$ is the generalized joint control vector. $\mathbf{b}$ is the bias term which contains the coriolis and gravity effects. H_{ij} for $(i, j) \in \{1,2,3,4\}$ are sub-matrices of the robot inertia matrix. $\mathbf{u}_{\mathbf{E}_1}$ and $\mathbf{u}_{\mathbf{E}_2}$ are the net force and torque effects of the reaction forces on the robot body, $\mathbf{u}_{\mathbf{E_L}}$ and $\mathbf{u}_{\mathbf{E_R}}$ stand for the effect of reaction forces on the robot joints for the left and right legs, respectively. They are calculated by utilizing the measured external forces $\mathbf{F}_{\mathbf{E_L}}$ and $\mathbf{F}_{\mathbf{E_R}}$, respectively, from the contact force sensors assembled at the feet soles as:

$$\mathbf{u}_{\mathbf{E_m}} = \mathbf{J}_{\mathbf{m}}^{\mathbf{T}}(\mathbf{x})\mathbf{F}_{\mathbf{E_m}} , \quad (2)$$

where $\mathbf{J_m}$ is the Jacobian of the leg $\mathbf{m}$ with:

$$\mathbf{m} = \begin{cases} \mathbf{L} & left \\ \mathbf{R} & right \end{cases} . \quad (3)$$

The subscripts $(\ )_{\mathbf{L}}$ and $(\ )_{\mathbf{R}}$ stand for the left and right leg, respectively.

Referring to the last two rows in (1) and (2), the unknowns are $\ddot{\boldsymbol{\theta}}_{\mathbf{m}}$ and $\mathbf{u}_{\mathbf{F_m}}$ which is the required vector to be calculated or estimated. Here, the other variables are either measured or estimated using known methods [59-61]. Therefore, the biped model is reduced and filtered to avoid the explicit calculation of $\ddot{\boldsymbol{\theta}}_{\mathbf{m}}$. The obtained reduced filtered dynamic is used to calculate the filtered version of required vector $\mathbf{u}_{\mathbf{F_m}}$.

3. Friction Estimation

In the proposed approach, the joint friction estimation depends on the knowledge of the applied control torque at the joint and the transmitted torque to the link which can be sensed by the reaction forces. The transmission and frictional forces are internal forces. Then, (1) can be reduced to represent the active joints dynamics and reshaped in terms of friction as:

$$\begin{pmatrix} \mathbf{u}_{\mathbf{F_L}} \\ \mathbf{u}_{\mathbf{F_R}} \end{pmatrix} = \begin{pmatrix} \boldsymbol{\tau}_{\mathbf{L}} \\ \boldsymbol{\tau}_{\mathbf{R}} \end{pmatrix} + \begin{pmatrix} \mathbf{u}_{\mathbf{E_L}} \\ \mathbf{u}_{\mathbf{E_R}} \end{pmatrix} - \bar{\mathbf{H}} \begin{pmatrix} \dot{\boldsymbol{\omega}}_b \\ \ddot{\boldsymbol{\theta}}_{\mathbf{L}} \\ \ddot{\boldsymbol{\theta}}_{\mathbf{R}} \end{pmatrix} - \begin{pmatrix} H_{31} \\ H_{41} \end{pmatrix} \dot{\mathbf{v}}_b - \begin{pmatrix} \mathbf{b}_{\mathbf{L}} \\ \mathbf{b}_{\mathbf{R}} \end{pmatrix} \tag{4}$$

with:

$$\bar{\mathbf{H}} = \begin{pmatrix} H_{32} & H_{33} & 0 \\ H_{42} & 0 & H_{44} \end{pmatrix} . \tag{5}$$

From(4), one can see that the right hand-side is the response due to the torque transmitted to the manipulator's links from the total applied joint control torque $\boldsymbol{\tau}_{\mathbf{m}}$.

The basic idea is to compute the right hand-side of (4), however, the existence of the angular acceleration terms which are in most cases unmeasured directly imposes a challenge. The solution to this problem is reported in the literature. The use of the band limited periodic excitation trajectories is reported in [63] which is not always possible. The offline numerical differentiation [9] is used too; however, it is inapplicable in the real time applications. Another method depends on the filtered dynamic model [62, 64] which is adopted here. By using this method, the explicit calculation of the angular acceleration terms is avoided by filtering both sides of (4) using a proper stable filter. The first order filter transfer function $Z(s)$ with the constant σ is adopted here. It is expressed as:

$$Z(s) = \sigma \frac{1}{s+\sigma} , \tag{6}$$

with its impulse response:

$$z(t) = \ell^{-1}\left(Z(s)\right) = \sigma e^{-\sigma t} , \tag{7}$$

where $\ell^{-1}(.)$ is the Laplace inverse transform. The multiplication in the frequency domain is equivalent to the convolution in time domain, and since there are N joint equations in (4), each of them can be filtered by (6). Therefore, there will be N filters with impulse responses as:

$$\mathbf{z}(t) = \begin{bmatrix} \sigma_1 e^{-\sigma_1 t} & & 0 \\ & \ddots & \\ 0 & & \sigma_N e^{-\sigma_N t} \end{bmatrix} , \tag{8}$$

where σ_i $i = 1, 2, \ldots, N$ are the i^{th} joint filter constants. Then the filtered version of (4) is:

$$\int_0^t \mathbf{z}(t-\tau) \begin{pmatrix} \mathbf{u}_{\mathbf{F_L}} \\ \mathbf{u}_{\mathbf{F_R}} \end{pmatrix} d\tau = \int_0^t \mathbf{z}(t-\tau) \left(\begin{pmatrix} \boldsymbol{\tau}_{\mathbf{L}} \\ \boldsymbol{\tau}_{\mathbf{R}} \end{pmatrix} + \begin{pmatrix} \mathbf{u}_{\mathbf{E_L}} \\ \mathbf{u}_{\mathbf{E_R}} \end{pmatrix} \right) d\tau + \\ - \int_0^t \mathbf{z}(t-\tau) \left(\bar{\mathbf{H}} \begin{pmatrix} \dot{\boldsymbol{\omega}}_b \\ \ddot{\boldsymbol{\theta}}_{\mathbf{L}} \\ \ddot{\boldsymbol{\theta}}_{\mathbf{R}} \end{pmatrix} \right) d\tau \\ - \int_0^t \mathbf{z}(t-\tau) \left(\begin{pmatrix} H_{31} \\ H_{41} \end{pmatrix} \dot{\mathbf{v}}_b + \begin{pmatrix} \mathbf{b}_{\mathbf{L}} \\ \mathbf{b}_{\mathbf{R}} \end{pmatrix} \right) d\tau \tag{9}$$

The term $\int_0^t \mathbf{z}(t-\tau) \left(\bar{\mathbf{H}} \begin{pmatrix} \dot{\boldsymbol{\omega}}_b \\ \ddot{\boldsymbol{\theta}}_{\mathbf{L}} \\ \ddot{\boldsymbol{\theta}}_{\mathbf{R}} \end{pmatrix} \right) d\tau$ can be integrated by parts with $\dot{\boldsymbol{\theta}}_{\mathbf{L}}(0) = \dot{\boldsymbol{\theta}}_{\mathbf{R}}(0) = \dot{\boldsymbol{\omega}}_b(0) = 0$

and: $\mathbf{z}(0) = \boldsymbol{\sigma} = \begin{bmatrix} \sigma_1 & & 0 \\ & \ddots & \\ 0 & & \sigma_N \end{bmatrix}$ as:

$$\int_0^t \mathbf{z}(t-\tau) \left(\bar{\mathbf{H}} \begin{pmatrix} \dot{\boldsymbol{\omega}}_b \\ \ddot{\boldsymbol{\theta}}_{\mathbf{L}} \\ \ddot{\boldsymbol{\theta}}_{\mathbf{R}} \end{pmatrix} \right) d\tau = \boldsymbol{\sigma} \bar{\mathbf{H}} \begin{pmatrix} \boldsymbol{\omega}_b \\ \dot{\boldsymbol{\theta}}_{\mathbf{L}} \\ \dot{\boldsymbol{\theta}}_{\mathbf{R}} \end{pmatrix} - \\ \int_0^t \mathbf{z}(t-\tau) \dot{\bar{\mathbf{H}}} \begin{pmatrix} \boldsymbol{\omega}_b \\ \dot{\boldsymbol{\theta}}_{\mathbf{L}} \\ \dot{\boldsymbol{\theta}}_{\mathbf{R}} \end{pmatrix} - \dot{\mathbf{z}}(t-\tau) \bar{\mathbf{H}} \begin{pmatrix} \boldsymbol{\omega}_b \\ \dot{\boldsymbol{\theta}}_{\mathbf{L}} \\ \dot{\boldsymbol{\theta}}_{\mathbf{R}} \end{pmatrix} d\tau \tag{10}$$

then (9) is modified accordingly as:

$$\int_0^t \mathbf{z}(t-\tau) \begin{pmatrix} \mathbf{u}_{\mathbf{F_L}} \\ \mathbf{u}_{\mathbf{F_R}} \end{pmatrix} d\tau = -\boldsymbol{\sigma} \bar{\mathbf{H}} \begin{pmatrix} \boldsymbol{\omega}_b \\ \dot{\boldsymbol{\theta}}_{\mathbf{L}} \\ \dot{\boldsymbol{\theta}}_{\mathbf{R}} \end{pmatrix} \\ + \int_0^t \mathbf{z}(t-\tau) \left(\begin{pmatrix} \boldsymbol{\tau}_{\mathbf{L}} \\ \boldsymbol{\tau}_{\mathbf{R}} \end{pmatrix} + \begin{pmatrix} \mathbf{u}_{\mathbf{E_L}} \\ \mathbf{u}_{\mathbf{E_R}} \end{pmatrix} + \dot{\bar{\mathbf{H}}} \begin{pmatrix} \boldsymbol{\omega}_b \\ \dot{\boldsymbol{\theta}}_{\mathbf{L}} \\ \dot{\boldsymbol{\theta}}_{\mathbf{R}} \end{pmatrix} - \begin{pmatrix} H_{31} \\ H_{41} \end{pmatrix} \dot{\mathbf{v}}_b - \begin{pmatrix} \mathbf{b}_{\mathbf{L}} \\ \mathbf{b}_{\mathbf{R}} \end{pmatrix} \right) d\tau \\ + \int_0^t \dot{\mathbf{z}}(t-\tau) \bar{\mathbf{H}} \begin{pmatrix} \boldsymbol{\omega}_b \\ \dot{\boldsymbol{\theta}}_{\mathbf{L}} \\ \dot{\boldsymbol{\theta}}_{\mathbf{R}} \end{pmatrix} d\tau \tag{11}$$

All the terms are filtered using (6), except for the last term $\int_0^t \dot{\mathbf{z}}(t-\tau) \bar{\mathbf{H}} \begin{pmatrix} \boldsymbol{\omega}_b \\ \dot{\boldsymbol{\theta}}_{\mathbf{L}} \\ \dot{\boldsymbol{\theta}}_{\mathbf{R}} \end{pmatrix} d\tau$ which is filtered using:

$$Z_2(s) = \ell\{\dot{z}(t)\} = \ell\{-\sigma^2 e^{-\sigma t}\} = -\sigma^2 \frac{1}{s+\sigma} , \tag{12}$$

or in matrix form:

$$\mathbf{z}_2(t) = -\begin{bmatrix} \sigma_1^2 e^{-\sigma_1 t} & & 0 \\ & \ddots & \\ 0 & & \sigma_N^2 e^{-\sigma_N t} \end{bmatrix} \tag{13}$$

By introducing the notation $\langle \eta \rangle_\lambda$ to indicate that the term η is filtered using the filter λ, the filtered dynamic equation is:

$$\left\langle \begin{pmatrix} \mathbf{u}_{\mathbf{F_L}} \\ \mathbf{u}_{\mathbf{F_R}} \end{pmatrix} \right\rangle_{Z(s)} = \boldsymbol{\sigma} \xi_1 + \langle \xi_2 \rangle_{Z(s)} + \langle -\xi_1 \rangle_{Z_2(s)} , \tag{14}$$

where:

$$\xi_1 = -\bar{\mathbf{H}}\begin{pmatrix}\boldsymbol{\omega}_b \\ \dot{\boldsymbol{\theta}}_\mathbf{L} \\ \dot{\boldsymbol{\theta}}_\mathbf{R}\end{pmatrix}, \tag{15}$$

and:

$$\xi_2 = \begin{pmatrix}\boldsymbol{\tau}_\mathbf{L} \\ \boldsymbol{\tau}_\mathbf{R}\end{pmatrix} + \begin{pmatrix}\mathbf{u}_{\mathbf{E_L}} \\ \mathbf{u}_{\mathbf{E_R}}\end{pmatrix} + \dot{\bar{\mathbf{H}}}\begin{pmatrix}\boldsymbol{\omega}_b \\ \dot{\boldsymbol{\theta}}_\mathbf{L} \\ \dot{\boldsymbol{\theta}}_\mathbf{R}\end{pmatrix} - \begin{pmatrix}H_{31} \\ H_{41}\end{pmatrix}\dot{\mathbf{v}}_b - \begin{pmatrix}\mathbf{b}_\mathbf{L} \\ \mathbf{b}_\mathbf{R}\end{pmatrix}, \tag{16}$$

The cut-off frequency of the first order filter affect the results. Its value depends on the highest meaningful frequency in the measurements ($\mathbf{F_E}$ and $\dot{\mathbf{v}}_b$). The cut-off frequency value should be higher than the highest meaningful frequency, at the same time, it should be able to smooth the measurements and reject the other higher frequencies. Therefore, the cut-off frequency value must not be too high.

All of the right hand terms of (14) are known and can be computed. Then the estimated filtered joint friction is used for two purposes: friction compensation when the foot is in contact with the ground and friction model parameter identification. The identification process takes place whenever the foot is in the contact with the ground and thus the identification is adaptive. When the leg is swinging, the friction model with the identified parameters is used to the represent the friction behavior. Friction models differ in their characteristics [12, 65]; however, the model parameters can be identified using identification tools, like the Recursive Least Squares method (RLS) [66]. For the identification process, the joint angular velocity is measured and $\left\langle \mathbf{u}_{\mathbf{F_m}} \right\rangle_{Z(s)}$ is estimated from (14) when the foot is in contact.

4. Results

The simulations are carried on 12 Degrees of Freedom (DOF) biped model. It consists of a trunk which connects a two 6-DOF legs. Three joint axes are positioned at the hip, two joints are at the ankle and one at the knee (Figure 1). MATLAB simulink contains a-three -axes IMU which consists of three -axes accelerometer and three -axes gyroscope with contaminated noise. The force sensors are fixed at the feet soles. It is assumed to have four three-axes force sensors located at known positions with respect to the foot link frame [67].

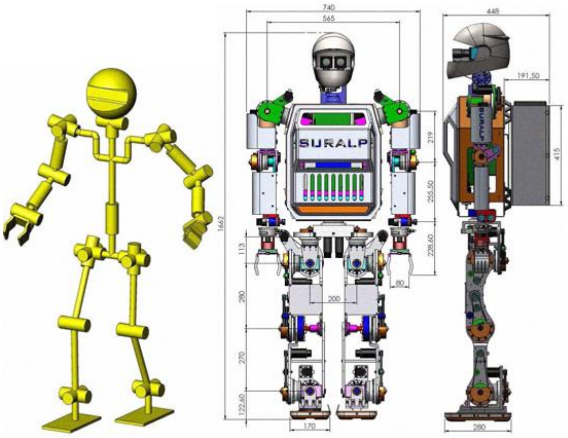

Figure 1. The kinematic arrangement and dimensional drawing of SURALP

To compare the true friction with the estimated one, the true friction values at the joints of the real biped have to be measured while walking. Therefore, only simulations are carried on the biped model and the true friction at the joint is generated using the nonlinear model [17]:

$$\mathbf{u_F} = \gamma_1\left(\underbrace{\tanh\left(\gamma_2\dot{\boldsymbol{\theta}}\right) - \tanh\left(\gamma_3\dot{\boldsymbol{\theta}}\right)}_{Stribeck\ effect}\right) + \underbrace{\gamma_4\tanh\left(\gamma_5\dot{\boldsymbol{\theta}}\right)}_{coulomb\ friction} + \underbrace{\gamma_6\dot{\boldsymbol{\theta}}}_{viscous\ dissipation} \tag{17}$$

where $\gamma_i, i = 1,\cdots,6$ are positive constants and the static coefficient of friction can be approximated by $\gamma_1 + \gamma_4$. **Note**: **This model is used solely as a joint friction generator.** The values of the parameters $\gamma_i, i = 1,\cdots,6$ for each joint of the leg are listed in Table 1 and generated true friction is the red line in Figure 3.

Figure 2 shows the walking trajectories, the walking starts after 0.5 sec, then the biped is in the left single support LS , DS then right single support RS and so forth.

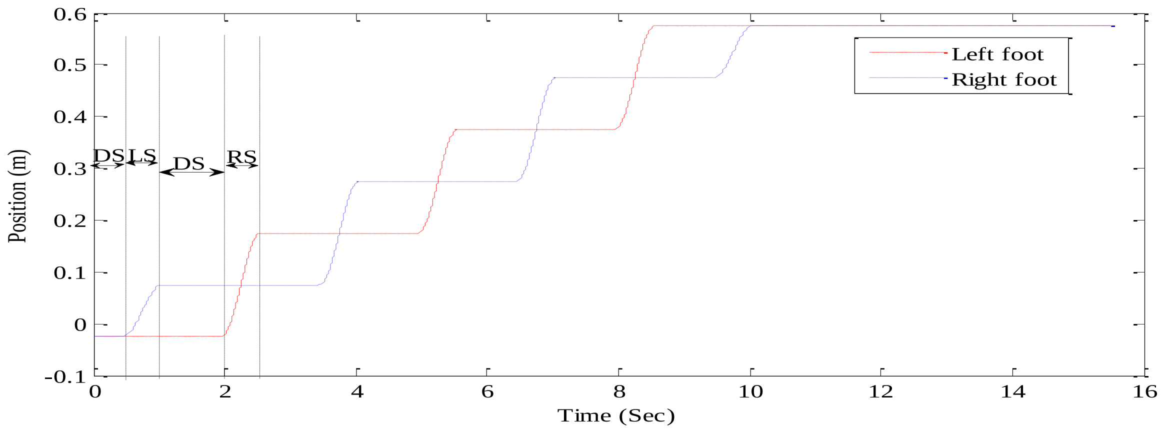

Figure 2. Feet walking trajectories, DS stands for the double support phase, LS stands for the left leg single support phase, and RS stands for the right leg single support phase

Table 1: True friction model parameters for each joint

	θ_1	θ_2	θ_3	θ_4	θ_5	θ_6
γ_1	0.7	0.6	0.5	0.4	0.2	0.05
γ_2	100	100	100	100	100	100
γ_3	10	10	10	10	10	10
γ_4	0.6	0.5	0.4	0.3	0.02	0.01
γ_5	100	100	100	100	100	100
γ_6	0.9	0.9	0.9	0.9	0.9	0.9

4.1. Model-Based Joint Friction Estimation

To be more realistic, the model-based friction estimation adopts another model differs from (17). For the joint $n, | n = 1, \ldots, 6$, the model is written as:

$$\left\langle \mathbf{u}_{\mathbf{F}_m}^n \right\rangle_{Z(s)} = F_c^n \operatorname{sgn}\left(\dot{\theta}_n\right) + F_v^n \dot{\theta}_n \quad , \tag{18}$$

Or for the joints of the leg $\mathbf{m}$:

$$\left\langle \mathbf{u}_{\mathbf{F}_m} \right\rangle_{Z(s)} = \begin{bmatrix} \operatorname{sgn}\left(\dot{\theta}_1\right) & 0 & 0 & \dot{\theta}_1 & 0 & 0 \\ 0 & \ddots & 0 & 0 & \ddots & 0 \\ 0 & 0 & \operatorname{sgn}\left(\dot{\theta}_6\right) & 0 & 0 & \dot{\theta}_6 \end{bmatrix}_{6\times 12} \begin{bmatrix} F_c^1 \\ \vdots \\ F_c^6 \\ F_v^1 \\ \vdots \\ F_v^6 \end{bmatrix} \tag{19}$$

where F_v and F_c are the viscous friction coefficient the coulomb friction, respectively. The estimated $\left\langle \mathbf{u}_{\mathbf{F}_m} \right\rangle_{Z(s)}$ from (14) is utilized in to estimate F_c^n and F_v^n when the leg is in contact based on the RLS algorithm. On the other hand, the friction behavior is represent by the estimated parameters $\hat{F}_v^n$ and $\hat{F}_c^n$ for each joint when the leg is swinging.

4.2. Measurement-Based Joint Friction Estimation

The estimation process of the joint friction is carried out simultaneously. Each joint of the two lgs has the same adopted friction model. The used filter constants are listed in

Table **2** and the estimated filtered friction is based on (14). The biped starts with the DS phase for 0.5 sec, during this period the friction estimation is measurement-based using (14). The resulted estimated filtered friction is used for the parameter identification process of the friction model parameters F_v^n and F_c^n. Once the biped switches to the LS phase, the friction behavior for the right leg joints is represented by the friction models with the identified parameters $\hat{F}_v^n$ and $\hat{F}_c^n$. Meanwhile, for the left leg joints, the estimation method is measurement-based and the corresponding friction models parameters are being identified. Later at the time instant t=1.1 sec, the estimation method is measurement-based and the friction model parameters are identified for both legs since the biped switches to the DS phase. Hence the identified parameters $\hat{F}_v^n$ and $\hat{F}_c^n$ for the right leg are re-identified and corrected. The biped switched to the RS phase at the time instant t=2 sec. Accordingly, the estimation process is measurement-based for the right leg joints and the parameter F_v^n and F_c^n are being identified. On the other hand, the identified parameters $\hat{F}_v^n$ and $\hat{F}_c^n$ of the left leg joints are used to represent the friction through the adopted friction models, and so forth.

Figure 3 shows both the true friction trajectory (dashed red line) and the estimated filtered friction (solid blue line) for the left leg. The true friction trajectory is generated using (17) with the parameters listed in Table 1. When the leg is swinging, the estimated friction uses the model (19) with the identified parameters. In these simulations, small and large frictional forces are used to test the ability of the proposed method. As depicted in Figure 3, the estimated filtered friction tracks the true friction. The present work differs from the work which is proposed by the authors in [60]. The differences lie in the facts that the present work does not assume the non-slipping case of the walking biped (therefore, it avoids the numerical errors of the pseudo inverse) and that the estimated filtered friction estimation is smoother in the present work.

Table 2. Filter constants

	θ_1	θ_2	θ_3	θ_4	θ_5	θ_6
σ	1	1	1	2	4	2

5. Conclusion

The joint friction of walking bipeds is estimated by combining the measurement-based method with the adaptive model-based method. The measurement-based estimation employs the biped reduced filtered dynamical model to compute the online filtered friction when the foot is in contact. It is based on readings of IMU and GRF. The dynamical model is filtered to avoid the explicit calculation of the joint angular accelerations. On the other hand, the adaptive model-based friction employs a friction model to represent the friction behavior when the leg is swinging. The model parameters are identified whenever the foot is in contact with the ground.

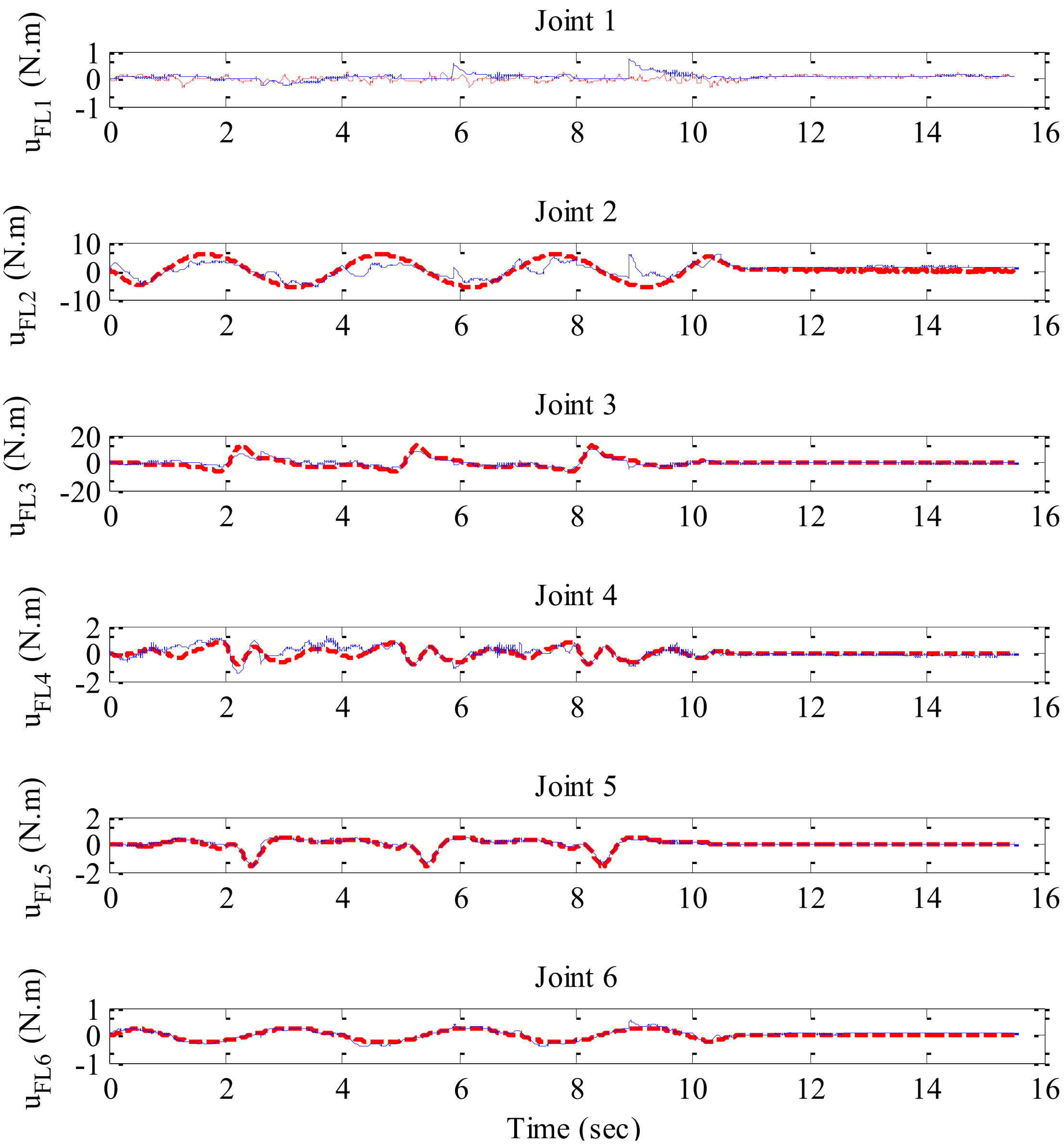

Figure 3: The estimated friction (solid blue line) and the true generated friction (dashed red line) for the left leg joints

References

[1] M. Koeda, Y. Uda, S. Sugiyama, T. Yoshikawa, "Shuffle turn and translation of humanoid robots". IEEE International Conference on Robotics and Automation (ICRA), Shanghai, 2011.

[2] K. Miura, S. Nakaoka, M. Morisawa, F. Kanehiro, K. Harada, S. Kajita, "Analysis on a friction based “Twirl” for biped robots". IEEE International Conference on Robotics and Automation (ICRA), Alaska, USA, 2010.

[3] S. Kajita, M. Morisawa, K. Miura, S. Nakaoka, K. Harada, K. Kaneko, F. Kanehiro, K. Yokoi, "Biped walking stabilization based on linear inverted pendulum tracking". IEEE/RSJ International Conference on Intelligent Robots and Systems (IROS), Taipei, Taiwan, 2010.

[4] T. Liu, Y. Inoue, K. Shibata, "A wearable ground reaction force sensor system and its application to the measurement of extrinsic gait variability". Sensors, Vol. 10, No. 11, 2010, 10240-10255.

[5] U. Seven, T. Akbas, K. Fidan, K. Erbatur, "Bipedal robot walking control on inclined planes by fuzzy reference trajectory modification". Soft Computing, Vol. 16, No. 11, 2012, 1959-1976

[6] S. J. Yi, B. T. Zhang, D. Hong, D. D. Lee, "Practical bipedal walking control on uneven terrain using surface learning and push recovery". IEEE/RSJ International Conference on Intelligent Robots and Systems (IROS), San Francisco, CA, USA, 2011.

[7] K. Yeoun-Jae, L. Joon-Yong, L. Ju-Jang, "A balance control strategy of a walking biped robot in an externally applied force". International Conference on Information and Automation (ICIA), Shenyang, China, 2012.

[8] J. P. Ferreira, M. M. Crisostomo, A. P. Coimbra, "Human Gait Acquisition and Characterization". IEEE Transactions on Instrumentation and Measurement, Vol. 58, No. 9, 2009, 2979-2988.

[9] B. Siciliano, O. Khatib. Springer Handbook of Robotics. Springer-Verlag New York, Inc. 2007.

[10] R. H. Hensen, M. Van de Molengraft, M. Steinbuch, "Friction induced hunting limit cycles: A comparison between the LuGre and switch friction model". Automatica, Vol. 39, No. 12, 2003, 2131-2137.

[11] H. Olsson, K. J. Astrom, "Friction generated limit cycles". IEEE Transactions on Control Systems Technology, Vol. 9, No. 4, 2001, 629-636.

[12] B. Bona, M. Indri, "Friction Compensation in Robotics: an Overview". IEEE European Control Conference on Decision and Control, Seville, Spain, 2005.

[13] F. Jatta, R. Adamini, A. Visioli, G. Legnani, "Hybrid force/velocity robot contour tracking: an experimental analysis of friction compensation strategies". IEEE International Conference on Robotics and Automation, Washington DC, 2002.

[14] B. Armstrong-Hélouvry, P. Dupont, C. C. De Wit, "A survey of models, analysis tools and compensation methods for the control of machines with friction". Automatica, Vol. 30, No. 7, 1994, 1083-1138.

[15] R. H. A. Hellsen, G. Z. Angelis, M. J. G. van de Molengraft, A. G. de Jager, J. J. Kok, "Grey-box Modeling of Friction: An Experimental Case-study". European Journal of Control, Vol. 6, No. 3, 2000, 258-267.

[16] V. Lampaert, J. Swevers, F. Al-Bender, "Modification of the Leuven integrated friction model structure". IEEE Transactions on Automatic Control, Vol. 47, No. 4, 2002, 683-687.

[17] C. Makkar, W. E. Dixon, W. G. Sawyer, G. Hu, "A new continuously differentiable friction model for control systems design". IEEE/ASME International Conference on Advanced Intelligent Mechatronics. Proceedings, Monterey, CA, 2005.

[18] R. H. A. Hensen, M. J. G. Van de Molengraft, M. Steinbuch, "Frequency domain identification of dynamic friction model parameters". IEEE Transactions on Control Systems Technology, Vol. 10, No. 2, 2002, 191-196.

[19] J. Moreno, R. Kelly, "Manipulator velocity field control with dynamic friction compensation". IEEE Conference on Decision and Control, Maui Hawaii, USA, 2003.

[20] J. Moreno, R. Kelly, R. Campa, "Manipulator velocity control using friction compensation". IEE Proceedings-Control Theory and Applications, Vol. 150, No. 2, 2003, 119-126.

[21] D. Kostic, B. de Jager, M. Steinbuch, R. Hensen, "Modeling and identification for high-performance robot control: an RRR-robotic arm case study". IEEE Transactions on Control Systems Technology, Vol. 12, No. 6, 2004, 904-919.

[22] G. Morel, K. Iagnemma, S. Dubowsky, "The precise control of manipulators with high joint-friction using base force/torque sensing". Automatica, Vol. 36, No. 7, 2000, 931-941.

[23] S. Grami, Y. Gharbia, "GMS friction compensation in robot manipulator". IEEE conference on Industrial Electronics Society (IECON), Vienna, Austria, 2013.

[24] Z. Dongdong, N. Jing, R. Xuemei, G. Herrmann, S. Longo, "Adaptive control of robotic servo system with friction compensation". IEEE Conference on Robotics, Automation and Mechatronics (RAM), 2011.

[25] L. R. Ray, A. Ramasubramanian, J. Townsend, "Adaptive friction compensation using extended Kalman–Bucy filter friction estimation". Control Engineering Practice, Vol. 9, No. 2, 2001, 169-179.

[26] P. Vedagarbha, D. M. Dawson, M. Feemster, "Tracking control of mechanical systems in the presence of nonlinear dynamic friction effects". IEEE Transactions on Control Systems Technology, Vol. 7, No. 4, 1999, 446-456.

[27] B. Friedland, Y. J. Park, "On adaptive friction compensation". IEEE Transactions on Automatic Control, Vol. 37, No. 10, 1992, 1609-1612.

[28] A. Mohammadi, M. Tavakoli, H. J. Marquez, F. Hashemzadeh, "Nonlinear disturbance observer design for robotic manipulators". Control Engineering Practice, Vol. 21, No. 3, 2013, 253-267.

[29] C. Wen-Hua, D. J. Ballance, P. J. Gawthrop, J. O'Reilly, "A nonlinear disturbance observer for robotic manipulators". IEEE Transactions on Industrial Electronics, Vol. 47, No. 4, 2000, 932-938.

[30] D. Xing, J. Su, Y. Liu, J. Zhong, "Robust approach for humanoid joint control based on a disturbance observer". Control Theory & Applications, IET, Vol. 5, No. 14, 2011, 1630-1636.

[31] J.-H. Ryu, J. Song, D.-S. Kwon, "A nonlinear friction compensation method using adaptive control and its practical application to an in-parallel actuated 6-DOF manipulator". Control Engineering Practice, Vol. 9, No. 2, 2001, 159-167.

[32] B. Armstrong, D. Neevel, T. Kusik, "New results in NPID control: Tracking, integral control, friction compensation and experimental results". IEEE Transactions on Control Systems Technology, Vol. 9, No. 2, 2001, 399-406.

[33] V. Lampaert, J. Swevers, F. Al-Bender, "Comparison of model and non-model based friction compensation techniques in the neighbourhood of pre-sliding friction". Proceedings of the American Control Conference, Boston, Massachusetts, 2004.

[34] S. N. Huang, K. K. Tan, T. H. Lee, "Adaptive friction compensation using neural network approximations". IEEE Transactions on Systems, Man, and Cybernetics, Part C: Applications and Reviews, Vol. 30, No. 4, 2000, 551-557.

[35] V. Vitiello, A. Tornambe, "Adaptive compensation of modeled friction using a RBF neural network approximation". IEEE Conference on Decision and Control, New Orleans, LA, 2007.

[36] Y. H. Kim, F. L. Lewis, "Reinforcement adaptive learning neural network based friction compensation for high speed and precision". Proceedings of the IEEE Conference on Decision and Control, Tampa, Florida USA, 1998.

[37] Y. F. Wang, D. H. Wang, T. Y. Chai, "Modeling and control compensation of nonlinear friction using adaptive fuzzy systems". Mechanical Systems and Signal Processing, Vol. 23, No. 8, 2009, 2445-2457.

[38] L. Mostefai, M. Denai, S. Oh, Y. Hori, "Optimal Control Design for Robust Fuzzy Friction Compensation in a Robot Joint". IEEE Transactions on Industrial Electronics, Vol. 56, No. 10, 2009, 3832-3839.

[39] W. Yongfu, W. Dianhui, C. Tianyou, "Extraction and Adaptation of Fuzzy Rules for Friction Modeling and Control Compensation". IEEE Transactions on Fuzzy Systems, Vol. 19, No. 4, 2011, 682-693.

[40] D. Velez-Diaz, T. Yu, "Adaptive robust fuzzy control of nonlinear systems". IEEE Transactions on Systems, Man, and Cybernetics, Part B: Cybernetics, Vol. 34, No. 3, 2004, 1596-1601.

[41] M. A. Llama, R. Kelly, V. Santibanez, "Stable computed-torque control of robot manipulators via fuzzy self-tuning". IEEE Transactions on Systems, Man, and Cybernetics, Part B: Cybernetics, Vol. 30, No. 1, 2000, 143-150.

[42] K. Shiev, N. Shakev, A. V. Topalov, S. Ahmed, "Trajectory control of manipulators using type-2 fuzzy neural friction and disturbance compensator". IEEE International Conference Intelligent Systems (IS), Sofia, 2012.

[43] Y. Yousif, K. Daws, B. Kazem, "Prediction of friction stir Welding characteristic using neural network". Jordan Journal of Mechanical and Industrial Engineering, Vol. 2, No. 3, 2008,

[44] B. S. Reddy, J. S. Kumar, K. V. K. Reddy, "Prediction of surface roughness in turning using adaptive neuro-fuzzy inference system". Jordan Journal of Mechanical and Industrial Engineering, Vol. 3, No. 4, 2009, 252-259.

[45] G. L. Wang, Y. F. Li, D. X. Bi, "Support Vector Networks in Adaptive Friction Compensation". IEEE Transactions on Neural Networks, Vol. 18, No. 4, 2007, 1209-1219.

[46] D. Vischer, O. Khatib, "Design and development of high-performance torque-controlled joints". IEEE Transactions on Robotics and Automation, Vol. 11, No. 4, 1995, 537-544.

[47] L. E. Pfeffer, O. Khatib, J. Hake, "Joint torque sensory feedback in the control of a PUMA manipulator". IEEE Transactions on Robotics and Automation, Vol. 5, No. 4, 1989, 418-425.

[48] C. S. L. Y. C. Toyota Technological Institute, "ICM13 Kana Kotaka et al," 2012.

[49] B. Ugurlu, T. Kawasaki, M. Kawanishi, T. Narikiyo, "Continuous and dynamically equilibrated one-legged running experiments: Motion generation and indirect force feedback control". International Conference on Intelligent Robots and Systems (IROS), Vilamoura, Algarve, Portugal, 2012.

[50] B. Ugurlu, I. Havoutis, C. Semini, D. G. Caldwell, "Dynamic trot-walking with the hydraulic quadruped robot- HyQ: Analytical trajectory generation and active compliance control". International Conference on Intelligent Robots and Systems (IROS), Tokyo, Japan, 2013.

[51] B. Ugurlu, K. Kotaka, T. Narikiyo, "Actively-compliant locomotion control on rough terrain: Cyclic jumping and trotting experiments on a stiff-by-nature quadruped". IEEE International Conference on Robotics and Automation (ICRA), Karlsruhe, Germany, 2013.

[52] H. Yan, B. Vanderborght, R. Van Ham, W. Qining, M. Van Damme, X. Guangming, D. Lefeber, "Step Length and Velocity Control of a Dynamic Bipedal Walking Robot With Adaptable Compliant Joints". IEEE/ASME Transactions on Mechatronics, Vol. 18, No. 2, 2013, 598-611.

[53] P. van Zutven, D. Kostic, H. Nijmeijer, "Foot placement for planar bipeds with point feet". IEEE International Conference on Robotics and Automation (ICRA), Saint Paul, Minnesota, USA, 2012.

[54] T. Hase, H. Qingjiu, C. Xuedong, "Performance analysis of biped walking robot with circular feet using optimal trajectory planning method". IEEE International Conference on Robotics and Biomimetics, Bangkok, Thailand, 2009.

[55] K. Miyahara, Y. Harada, D. N. Nenchev, D. Sato, "Three-dimensional Limit Cycle Walking with joint actuation". IEEE/RSJ International Conference on Intelligent Robots and Systems (IROS), Louis, USA, 2009.

[56] K. Joohyung, K. Hoseong, L. Heekuk, S. Keehong, L. Bokman, L. Minhyung, L. Jusuk, R. Kyungsik, "Balancing control of a biped robot". IEEE International Conference on Systems, Man, and Cybernetics (SMC), Seoul, Korea, 2012.

[57] T. Yoshikawa, O. Khatib, "Compliant humanoid robot control by the torque transformer". IEEE/RSJ International Conference on Intelligent Robots and Systems (IROS), Louis, USA, 2009.

[58] S. I. Han, K. S. Lee, "Robust friction state observer and recurrent fuzzy neural network design for dynamic friction compensation with backstepping control". Mechatronics, Vol. 20, No. 3, 2010, 384-401.

[59] I. Hashlamon, K. Erbatur, *Experimental verification of an orientation estimation technique for autonomous robotic platforms*, Master thesis, Sabanci University, 2010.

[60] I. Hashlamon, K. Erbatur, "Joint friction estimation for walking bipeds". Robotica, Vol. 34, No. 7, 2014, 1610-1629.

[61] I. Hashlamon, K. Erbatur, "Center of Mass States and Disturbance Estimation for a Walking Biped ". IEEE International Conference on Mechatronics (ICM 2013), Vicenza, Italy, 2013.

[62] M. Van Damme, P. Beyl, B. Vanderborght, V. Grosu, R. Van Ham, I. Vanderniepen, A. Matthys, D. Lefeber, "Estimating robot end-effector force from noisy actuator torque measurements". IEEE International Conference on Robotics and Automation (ICRA), Shanghai, 2011.

[63] J. Swevers, C. Ganseman, D. B. Tukel, J. De Schutter, H. Van Brussel, "Optimal robot excitation and identification". IEEE Transactions on Robotics and Automation, Vol. 13, No. 5, 1997, 730-740.

[64] P. Hsu, M. Bodson, S. Sastry, B. Paden, "Adaptive identification and control for manipulators without using joint accelerations". Proceedings IEEE International Conference on Robotics and Automation, Raleigh, NC, USA, 1987.

[65] H. Olsson, K. J. Åström, C. Canudas de Wit, M. Gäfvert, P. Lischinsky, "Friction models and friction compensation". European journal of control, Vol. 4, No. 1998, 176-195.

[66] L. Ljung. System Identification: Theory for the User. 2nd. Upper Saddle River, NJ: Prentice-Hall PTR. 1999.

[67] K. Erbatur, U. Seven, E. Taskiran, O. Koca, M. Yilmaz, M. Unel, G. Kiziltas, A. Sabanovic, A. Onat, "SURALP: A New Full-Body Humanoid Robot Platform". IEEE-Rsj International Conference on Intelligent Robots and Systems, New York, 2009.